Chapter

Performance Evaluation and Mechanism Study of a Silicone Hydrophobic Polymer for Improving Gas Reservoir Permeability

Jie Zhang, Xu-Yang Yao, Bao-Jun Bai and Wang Ren

Abstract

The permeability of tight gas reservoirs is usually lower than 1 md. When the external fluids from drilling and completion processes invade such reservoirs, formation damage occurs and causes serious damage to oil and gas production. Fluorocarbon surfactants are most often recommended for removing such damage because they have extremely low surface tension, which means that they can change the reservoir wettability from water wet to gas or oil wet. However, they are not normally applied in the field because they are not cost-effective. Besides, some environmental concerns also restrict their application. In this work, we studied the effects of an oligomeric organosilicon surfactant (OSSF) on wettability modification, surface tension reduction, invasion of different fluids, and fluid flow back. It was found that the amount of spontaneous imbibition and remaining water could be reduced by the surfactant as a result of surface tension reduction and wettability alteration. Compared to the distilled water, the concentration of 0.20 wt% OSSF could decrease water saturation of cores by about 4%. At a flow-back pressure of 0.06 and 0.03 MPa after 20 PV displacement, permeability recovery could increase from 8 to 7–93% and 86%, respectively. We also found that the mechanism of OSSF includes the physical obstruction effect, surface tension reduction of external fluids, and wettability alteration of the reservoir generated. Meanwhile, quantum chemical calculations indicated that adsorbent layer of polydimethylsiloxane could decrease the affinity and adhesion of CH_4 and H_2O on the pore surface.

Keywords: low-permeability reservoir, silicone hydrophobic polymer, spontaneous imbibition, antiwater blocking, water saturation, gas permeability improvement

1. Introduction

Water blocking can damage the low permeability of a normally tight gas reservoir due to the increase of water saturation and the reduction of gas phase permeability in the process of drilling, completion, and stimulation. Zhong et al. [1] showed that the permeability damage rate in a gas reservoir could reach 70–90%, and the gas well production could decrease by more than 70% when water-blocking

damage occurred. Therefore, it is important to develop an antiwater blocking agent with high efficiency and low cost for the development of a superior low-permeability gas reservoir.

At present, most researchers consider water blocking as caused by capillary thermodynamics and dynamics [2]. The commonly used antiwater blocking agents include lower alcohol content agents (especially methanol), alcohol ethers, silyl ethers, hydrocarbon surfactants [3], and fluorocarbon surfactants, and "... the alcohols react with formation water in the reservoir to form low boiling point azeotrope, which is helpful for gasification and flow back of the injected water" [4]. Nasr et al. indicated that the glycol ether and polyethylene glycol monobutyl ether could remove the water blocking damage and improve the permeability of oil fields in Arab countries [5]. Zhang et al. evaluated the effects of methanol, ethanol, and ethylene glycol on alleviating the water blocking damage of the low-permeability sandstone gas reservoir. The results showed that methanol had the most favorable performance, followed by ethanol and ethylene glycol, respectively [6]. "Bai et al. compared the anti-water blocking effects of methanol and petroleum sulfonate on a low permeability gas reservoir and found methanol to have better performance ... " Surfactants can reduce the surface tension and change the reservoir wettability from water wetting to gas or oil wetting [7]. Bang et al. reduced the water blocking damage and increased the fluid flow in the fracture reservoirs with an alcohol solution containing a fluorocarbon surfactant. They also reduced the water blocking damage of the condensate in gas reservoirs by applying the fluorocarbon surfactant. The results showed that the hydrated silanol groups could adsorb water from pore surfaces via covalent bonding with the alkenyl groups of fluorocarbon surfactants. This made fluorine-containing alkyl directionally arranged, changing the reservoir wettability from water wetting to oil wetting and finally increasing the gas phase permeability [8–10]. Li et al. developed an antiwater blocking agent containing perfluoroalkyl side chains by using a stepwise emulsion polymerization method, which showed low surface tension and interfacial tension. The surfactant can adsorb on the surface of the pore via chemical adsorption and modify the surface to preferential gas wetting [11]. Li et al. used two nonionic fluorocarbon surfactant methanol solutions for water phase displacement experiments and found that it could improve the permeability [12]. Liu et al. synthesized a cationic fluoride Gemini surfactant and recorded ultralow surface tension; moreover, its solution could remarkably reduce the damage of water blocking on low-permeability formations [13]. Liu et al. found that a wettability variation from water wetting to gas wetting was achieved by adding 0.1 wt% fluoride. The core flow tests indicated that both the flow back rate and gas relative permeability were significantly improved [14]. Biosurfactants such as *Sophora japonica*, trehalose lipid, rhamnolipid, peptide, and some polymer surfactants also show good prospects in relieving water blocking damage because they can change the wettability by adding a large amount of active groups adsorbed on the rock surface. Moreover, they are natural, environmentally friendly, and easy to produce in the industry. Zhang prepared a biosurfactant referred to as the stearic acid glucose ester methoside maleic acid diester, which can decrease the interfacial tension and overcome the water blocking effect. It has good thermal stability and chemical stability [15].

Due to the high cost and environment concerns of fluorocarbon surfactants, an oligomeric organosilicon surfactant (OSSF) contained functional groups such as the silicon hydroxyl group. The silicon oxygen chain and silicon methyl were prepared by polycondensation reaction [16]. Gas preferential wettability could be achieved by oriented adsorption of silicon methyl via hydrogen bonding or chemical condensation. It could also decrease the dynamic surface tension of fluids owing to faster interfacial adsorption of small molecules during diffusion adsorption.

DOI: http://dx.doi.org/10.5772/intechopen.90811

Besides, it possesses super-strong surface activity, and a very small amount can decrease the surface tension to less than 25 mN/m, while the cost is less than 1/10 of fluorocarbon surfactants.

In this study, the influence of OSSF on the aqueous phase trapping damage was evaluated through the measurement of spontaneous imbibition distilled water saturation, water blocking damage rate, permeability recovery, and remaining water saturation. The mechanisms were explained using aggregates blocking, directional adsorption, wettability alteration, and quantum chemistry calculations.

2. Experimental approach

2.1 Materials

2.1.1 Surfactants

In this study, OSSF and ABSN were used to alleviate the aqueous phase trapping damage to low-permeability sand formation. Both surfactants are water soluble and transparent liquids and were made in our laboratory. The relative molecular mass of an OSSF is 2000–3000. It includes a hydrophobic group of permethylated siloxane, hydrophilic groups of sulfonic acid groups, and hydroxyls. The polydimethylsilioxane chain enables the surfactant to have water-repelling characteristics and low surface tension. These properties enable its adsorption on the rock via multiple points of attachment and give the surfactant a long-term effectiveness. ABSN is quaternary ammonium salt cationic surfactant, and the hydrophobic tail is dodecyl benzene. **Figure 1(a)** and **(b)** shows the chemical structure of dodecyl benzene sulfonate triethanolamine (ABSN) and oligomeric organosilicon surfactant (OSSF), respectively. The artificial and reservoir cores used in the same experiment have the same composition and similar porosity and permeability.

2.1.2 Cores

The cores used in this study include artificial cores and reservoir cores. They have same compositions and similar porosity and permeability. The artificial cores (obtained from Haian Petroleum Scientific Research Instrument Co., Ltd. in Nantong, China) are mainly composed of quartz sand, which does not contain any water sensitive substance. Reservoir cores were drilled at the Yingxi exploratory area in the Qinghai oilfields. The physical characteristics of these cores are listed in **Table 1**.

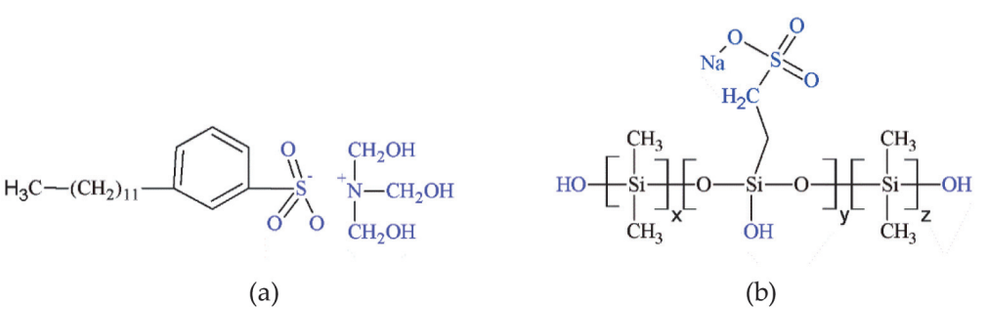

Figure 1.
Chemical structure of (a) ABSN and (b) OSSF.

Type	L/(mm)	D/(mm)	m/(g)	Φ/(%)	K/(10^{-3} μm^2)	Standard error	
						Φ	K
Artificial cores	50.89	24.77	54.83	14.69	28.59	0.66	0.48
Artificial cores	50.75	24.83	54.12	13.91	27.61	0.54	0.61
Artificial cores	50.92	24.81	53.72	15.27	29.86	0.67	0.52
Reservoir cores	51.02	24.95	62.67	0.67	3.27	0.49	0.57
Artificial cores	50.81	24.83	53.15	14.34	26.91	0.83	0.64
Artificial cores	49.95	24.94	54.27	14.76	28.95	0.70	0.67
Artificial cores	50.24	24.86	53.65	14.08	26.69	0.51	0.59

Table 1.
Physical characteristics of cores used in this study.

2.1.3 Fluids

Triply distilled water was used in all experiments. About 4% of sodium bentonite mud was added with 0.2% Na_2CO_3 and then stirred for 2 days. It was used as the basic mud. Sodium bentonite was obtained from Weifang Hua Bentonite Group Co., Ltd. Na_2CO_3 is a commercially pure reagent.

2.2 Experimental method

2.2.1 Determination of contact angle, wettability, and surface energy

Cores were immersed in NaOH solution with a pH of 9 at 150°C for 16 h. Each core was then taken out and dried at 150°C for 4 h. After that, it was cooled down to room temperature. The contact angles among the cores, distilled water, and ethylene glycol were measured with a JC200D3 contact angle analyzer. When the contact angle of water is less than 75°, it is termed "water wetting." When the contact angle of water is greater than 110°, it is considered "oil wetting" [17]. When the contact angle is between 75° and 110°, it is considered "intermediate wetting." This is a condition of gas preferential wetting. The surface energy of cores was calculated using the Owens-Wendt formula [18]. Aging in this paper means rolling under the high temperature of 150°C for 16 h.

2.2.2 Determination of surface tension

The surface tension measurements of NaOH solution with a pH of 9 and basic mud filtrates before and after aging (rolling in the temperature of 150°C oven for 16 h) were performed with an interfacial tensiometer sigma 701 (KSV, Finland) using the dynamic Wilhelmy plate method.

2.2.3 Spontaneous imbibition experiments

Figure 2 shows the experiment's core inside the core holder, and a certain confinement pressure was added. The distilled water was added into the metering tube followed by the OSSF solution. The initial contact volume of the liquid with cores was determined based on the different flow rates. The increased water saturation, defined as spontaneous imbibition volume divided by the core's pore volume, was recorded during the experiment [19]. Core permeability change rates

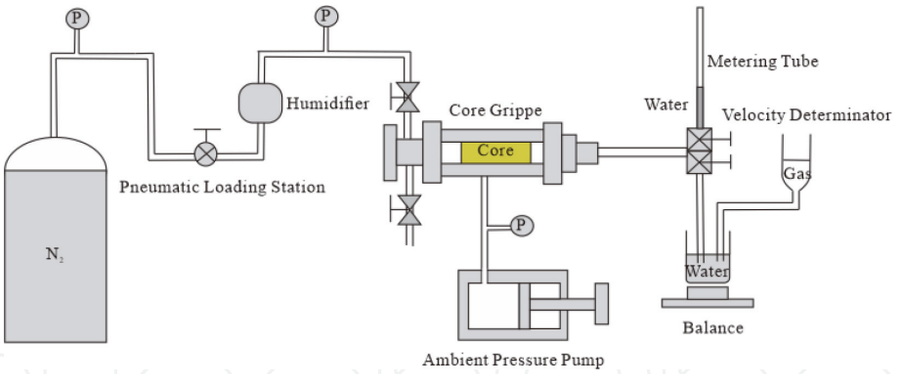

Figure 2.
Schematic of the apparatus used for spontaneous imbibition and reverse displacement.

at different times were defined as the water blocking damage rate. This rate can be calculated [20]:

$$\mathrm{I} = \frac{K_0 - K_i}{K_0} \times 100\% \tag{1}$$

where K_0 (10^{-3} μm^2) is the gas permeability of artificial cores with irreducible water saturation, and K_i (10^{-3} μm^2) is the gas permeability of artificial cores under different times.

2.2.4 Gas driven flow-back experiment

The cores were gas driven and saturated with flow-back spontaneous imbibition. They were used to weigh the core mass at different flow-back stages and to calculate the residual water saturation. The gas permeability recovery was calculated as follows [21, 22]:

$$D = \frac{K_{npv}}{K_0} \times 100\% \tag{2}$$

where K_0 (10^{-3} μm^2) is the gas permeability of artificial cores at irreducible water saturation established by the unsteady state gas drive. K_{nPV} (10^{-3} μm^2) is the gas permeability of artificial cores after they were displaced by gas; these cores represent the gas permeability during different flow-back stages.

3. Results and discussion

3.1 Wettability properties

This section presents an evaluation of the wettability alteration on both artificial cores and reservoir cores using different surfactants in alkaline solutions. Both the distilled water and ethylene glycol experiments were carried out under high temperatures. As shown in **Table 2** (**Figure 3**), water and ethylene glycol spreading on the artificial cores were treated by 0.2 and 0.4 wt% ABSN; thus, the contact angles were too low to measure. The contact angles of 0.2 wt% OSSF treated cores were 110.12° and 27.54°, respectively. Considering the microscopic anisotropy of the cores and the measurement error, we believe that the real contact angles should not

vary dramatically from one another. The surface energy of the cores decreased to 20–25 mJ/m^2, which indicated that OSSF could greatly change the wettability from hydrophilic to highly hydrophobic.

As shown in **Table 3** (**Figure 4**), the 0.2 and 0.4 wt% ABSN-treated cores displayed lower water contact angle, and the ethylene glycol droplet completely

Concentration/wt%	Contact angle/°		Surface energy/ (mJ/m^2)	Standard error		
	Distilled water	Ethylene glycol		Distilled water	Ethylene glycol	Surface energy
0.00	Droplet infiltration	Droplet infiltration	—	—	—	
0.20% ABSN	Droplet infiltration	Droplet infiltration	—	—	—	
0.40% ABSN	Droplet infiltration	Droplet infiltration	—	—	—	
0.20% OSSF	110.12	27.54	24.66	2.55	1.80	6.53
0.40% OSSF	110.71	32.14	22.83	2.49	1.84	5.76

Table 2.
Contact angle and surface energy of artificial cores after adsorption equilibrium in ABSN and OSSF solutions (T = 150°C, pH = 9).

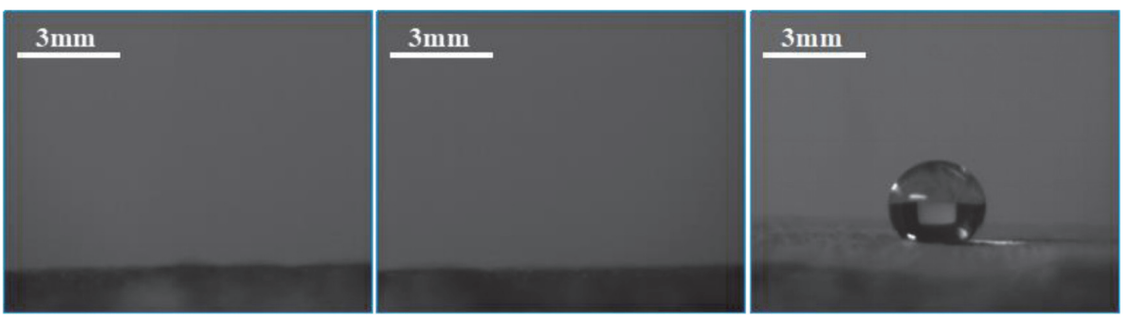

(a) (b) (c)

Figure 3.
Contact angle of water on artificial cores (room temperature). (a) Untreated, (b) treated by 0.20 wt% ABSN, and (c) treated by 0.20 wt% OSSF.

Concentration/wt%	Contact angle/ (°)		Surface energy/ (mJ/m^2)	Standard error		
	Distilled water	Ethylene glycol		Distilled water	Ethylene glycol	Surface energy
0.0	13.47	Droplet spreading	—	—	—	
0.20% ABSN	8.75	Droplet spreading	—	—	—	
0.40% ABSN	6.42	Droplet spreading	—	—	—	
0.20% OSSF	104.53	39.19	28.05	1.87	2.14	4.13
0.40% OSSF	107.48	48.50	26.49	1.33	2.39	1.32

Table 3.
Contact angle and surface energy of reservoir cores after adsorption equilibrium in ABSN and OSSF solutions (T = 150°C, pH = 9).

spread on the surface. However, the contact angle of water on the OSS-modified cores still reached 110°, and the surface energy decrease was between 26 and 28 mJ/m^2. These results indicated that water did not spread on the surface of the pore due to the formation of low energy adsorption film treated by OSSF. Since ABSN does not affect wettability alteration, its surface energy is not evaluated here.

3.2 Interfacial properties

To evaluate the surface activities of OSSF and ABSN in a high-temperature basic environment, the surface tension of solutions and fluid filtrates was measured after aging at 150°C for 16 h. In **Figures 5** and **6**, both 0.2–0.4 wt% ABSN and OSSF could decrease the surface tension under high temperature. Meanwhile, OSSF was better at reducing surface tension, meaning that it could better reduce filtrate adsorption and aqueous phase trapping damage in the rock.

3.3 Evaluation of antiwater blocking properties of OSSF

3.3.1 Spontaneous imbibition property of cores

As shown in **Figure 7**, water saturation of cores gradually increased with time. Obvious spontaneous imbibition and diffusion stages could also be seen. The increase in water saturation was dramatic at the spontaneous imbibition stage, but water

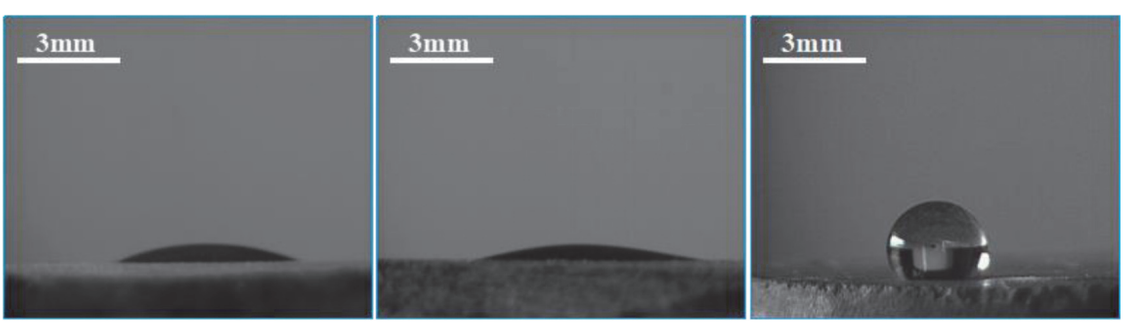

Figure 4.
Contact angle of water on reservoir cores (room temperature). (a) Untreated, (b) treated by 0.20 wt% ABSN, and (c) treated by 0.20 wt% OSSF.

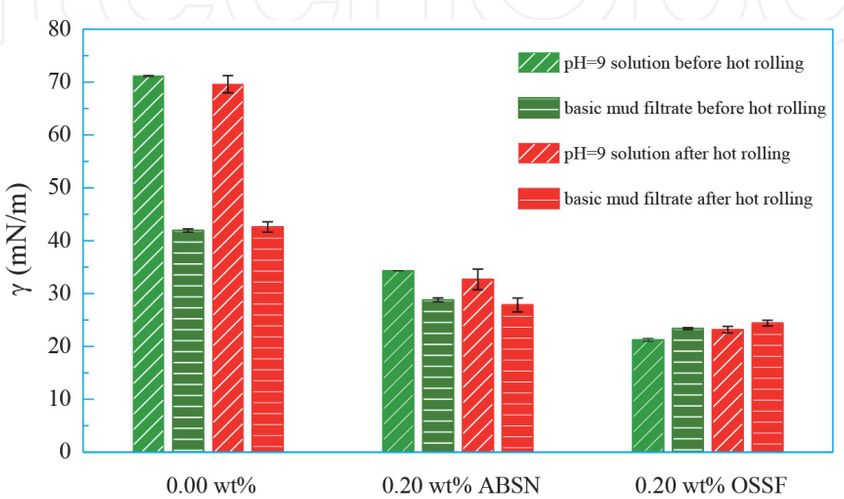

Figure 5.
Surface tension of 0.20 wt% solutions before and after aging (cooling down to room temperature, pH free).

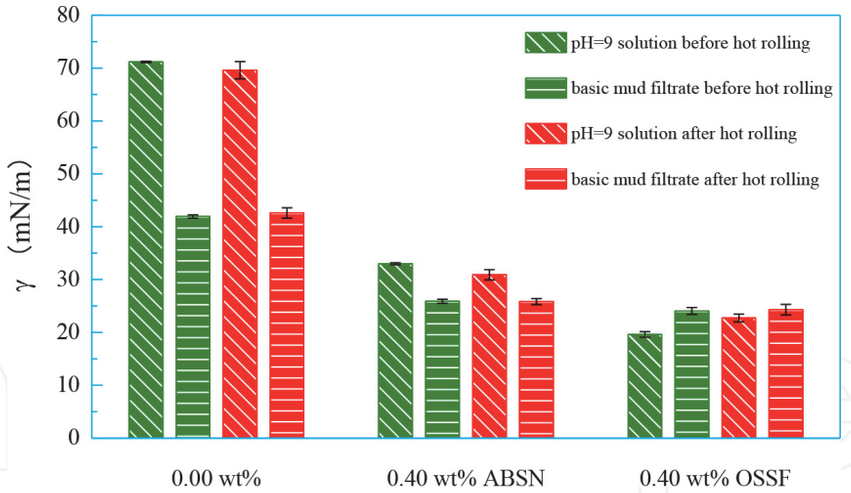

Figure 6.
Surface tension of 0.40 wt% solutions before and after aging (T = 25°C, pH free).

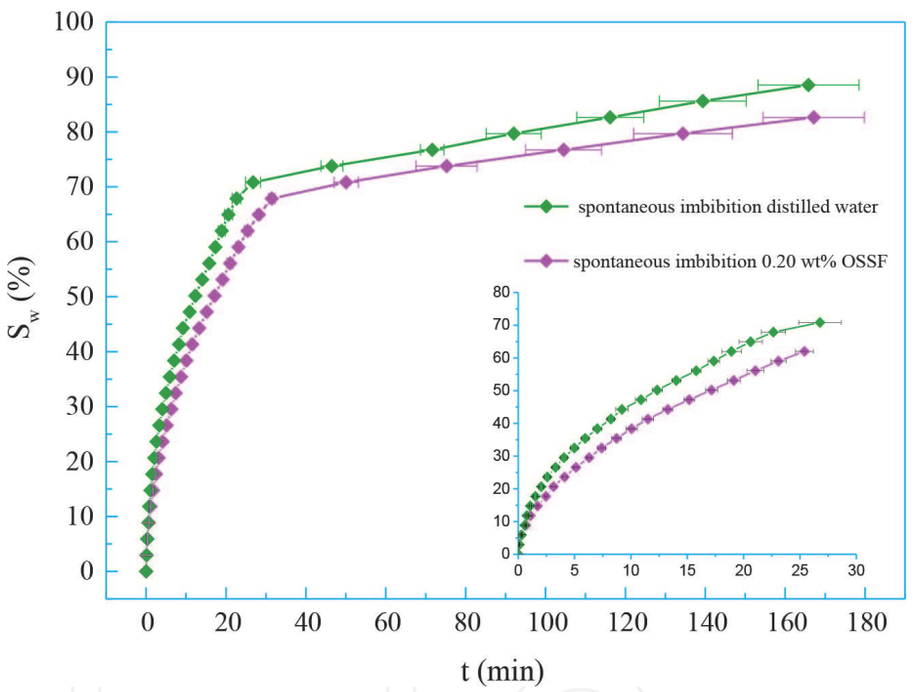

Figure 7.
Water saturation (S_w) of artificial cores versus spontaneous imbibition time (t).

saturation was compromised at the diffusion stage. Effective pores can imbibe the liquid by capillary force, whereas liquid accessing to unconnected pores only relies on diffusion from connected pores, which requires more time. Water saturation decreased from about 71–68% with a 0.20 wt% OSSF in the spontaneous imbibition stage. The spontaneous imbibition time then changed from about 33 to 28 min.

Figure 8 shows the cores treated by 0.2% OSSF solution. Water saturation decreased to 56% and the saturation time decreased to 68 min in the spontaneous imbibition stage. These results indicate that the spontaneous imbibition rate and the amount of external liquid in a reservoir can easily be reduced.

3.3.2 Water blocking damage rate of cores

As shown in **Figure 9**, the water blocking damage rate of distilled water and OSSF solutions increased sharply at the beginning. However, after 20 min, it slowly

started to increase. Compared with distilled water, OSSF solution could achieve an additional damage rate reduction of 15%. The results suggest that the water blocking damage rate of the reservoir increased remarkably when the external liquids invaded into reservoir at the beginning. After reaching a certain water saturation, the water blocking damage did not increase significantly.

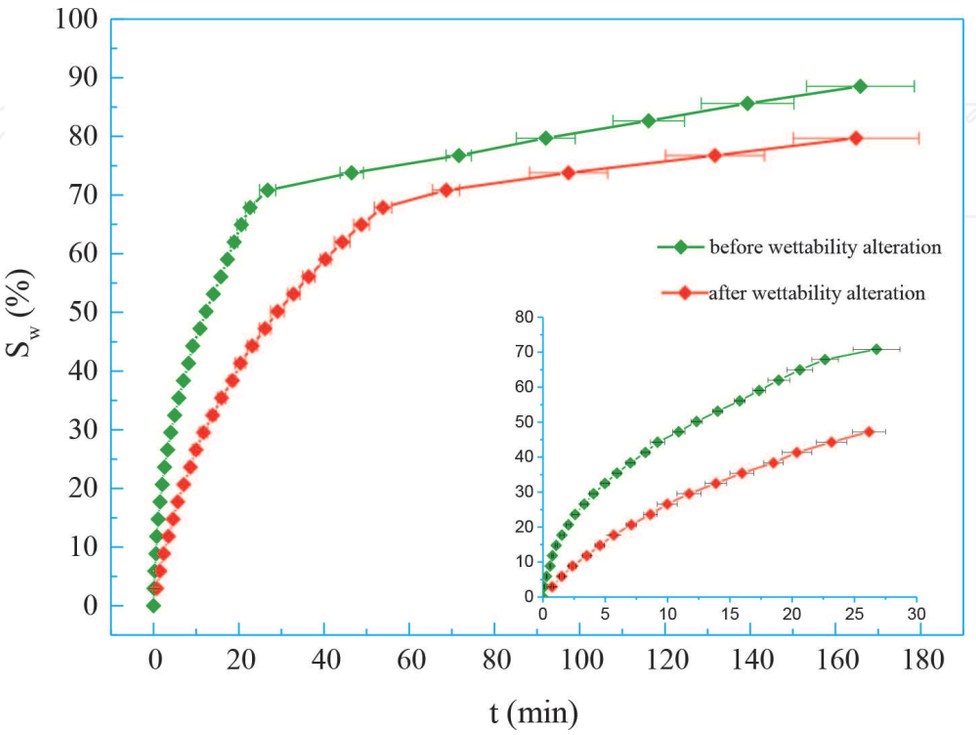

Figure 8.
Water saturation (S_w) of artificial cores treated by 0.2% OSSF solution.

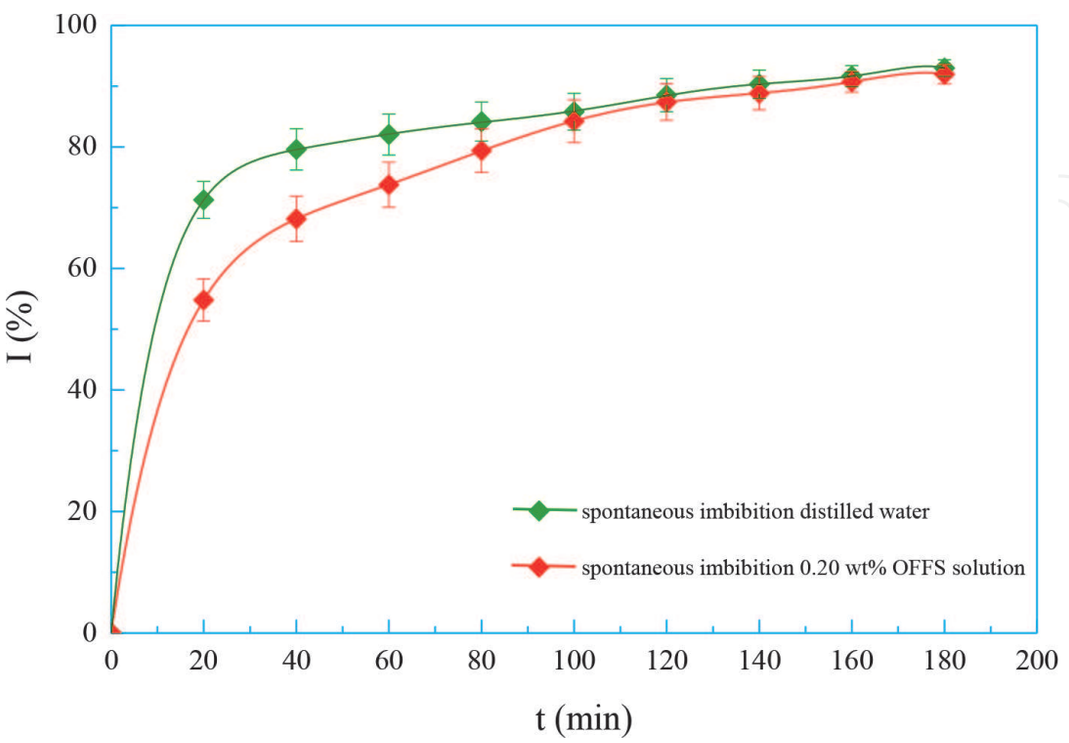

Figure 9.
Water blocking damage rate (I) of artificial cores versus self-absorbed time (t).

3.3.3 Permeability recovery of cores

As shown in **Figure 10**, the permeability recovery of the cores gradually increases with flow-back PV. Meanwhile, the recovery rate gradually decreases. When gas pressure was 0.06 MPa and the flow-back PV is 20, the cores' permeability recovery changes from 7 to 77%. It is evident that the higher the displacing pressure, the higher the permeability recovery. A permeability recovery of 0.20%

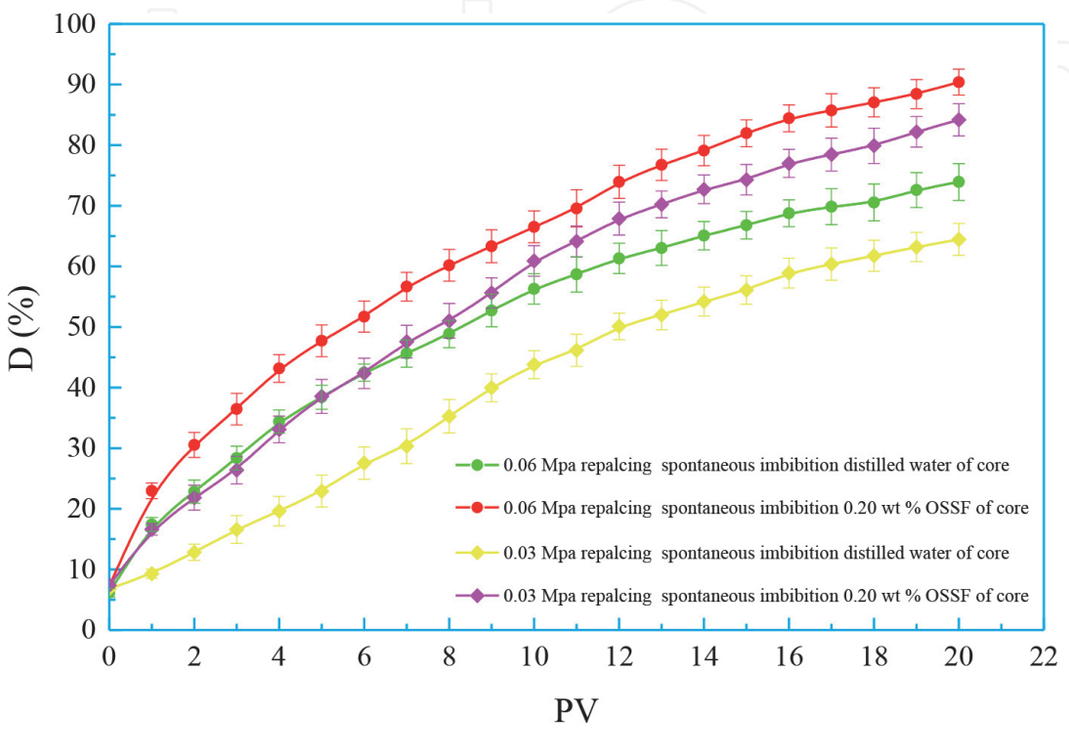

Figure 10.
Pore volumes (PV) versus permeability recovery rate of artificial cores (D).

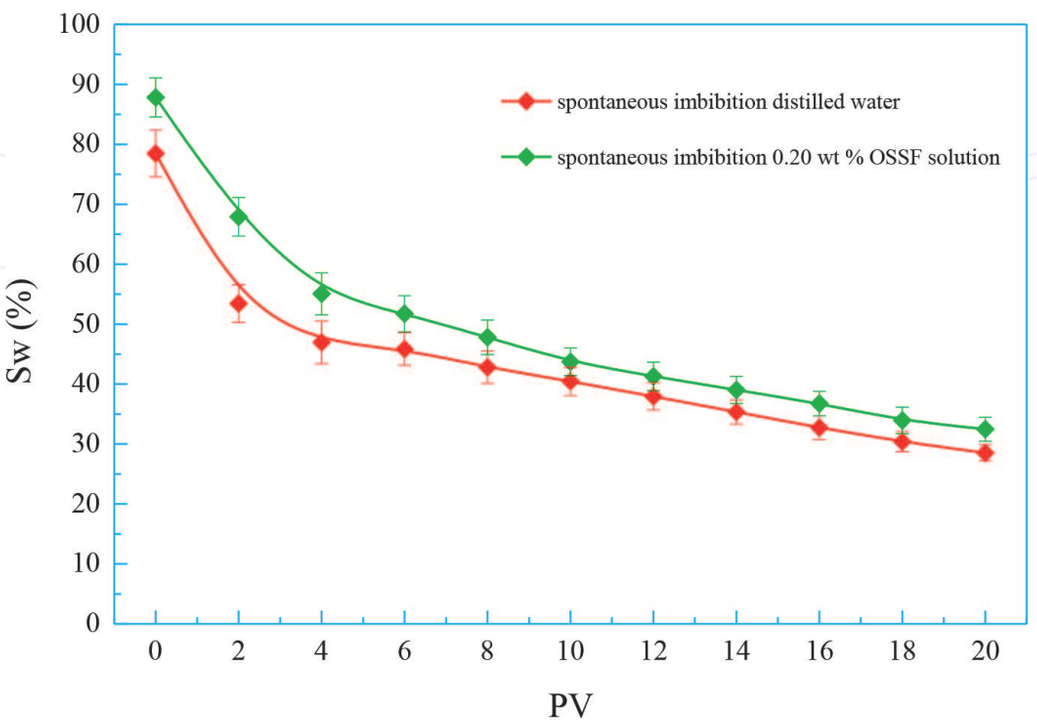

Figure 11.
Gas flow-back volumes versus remaining water saturation (S_w) of artificial cores.

OSSF solution increased from about 8 to 93%; then, with the distilled water, the permeability recovery was 77%. Both increases were at 0.06 MPa and 20 PV. At 0.03 MPa and 20 PV, permeability recovery of 0.20% OSSF solution increased from about 7 to 86%, with the distilled water 67% by contrast. These results illustrate that the increase of flow-back volume and gas pressure can improve the permeability recovery and reduce the water blocking damage of cores. In addition, OSSF is beneficial to the permeability recovery of the reservoirs damaged by external fluids.

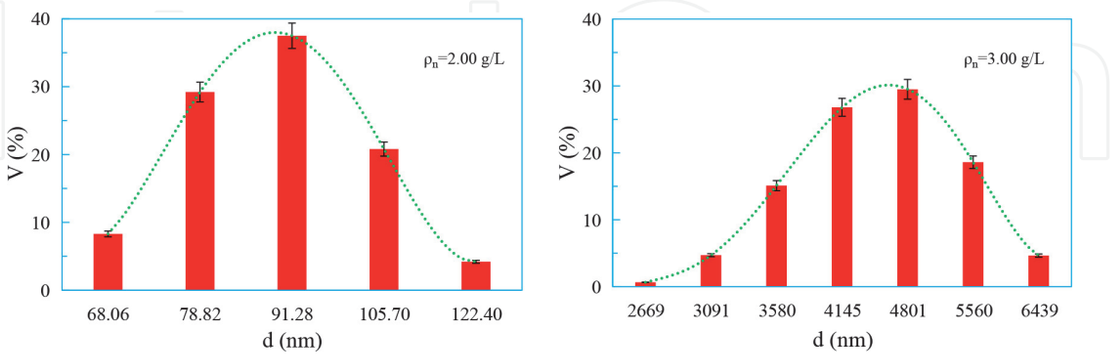

Figure 12.
Size and distribution of OSSF aggregate versus weight percentage (T = 25°C, free pH).

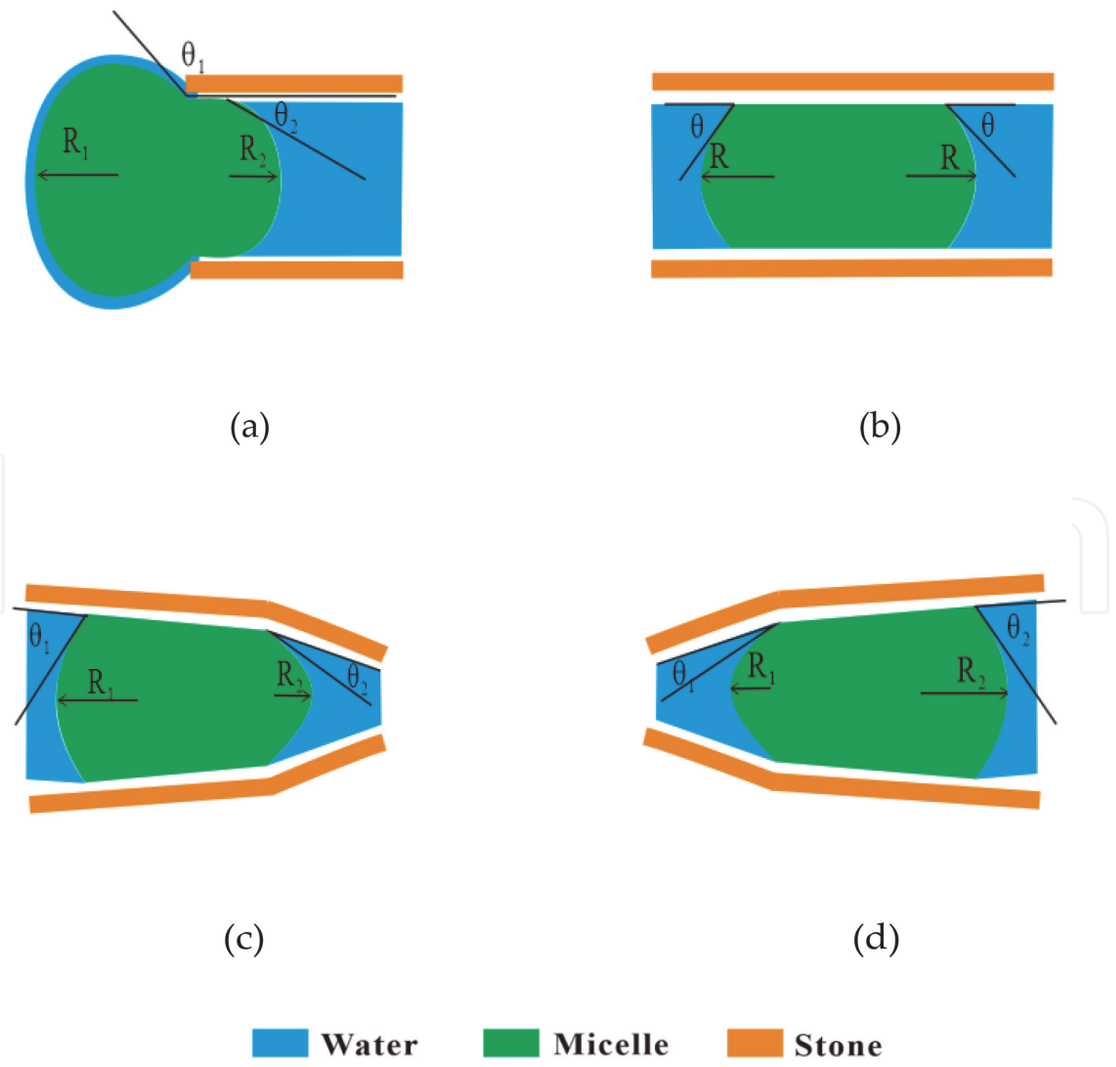

Figure 13.
Flow patterns of OSSF aggregate in the reservoir pores.

3.3.4 Retained water saturation of cores

Accumulation of external fluids in gas reservoir is the principle factor responsible for water blocking damage [23, 24]. As shown in **Figure 11**, the remaining water saturation decreased with PV, but the decreasing rate reduced gradually. Retained water saturation of 0.20% OSSF solution decreased from about 83 to 30%; moreover, with the distilled water, the water saturation decreased from 90 to 34% by contrast. The results reveal that increasing flow-back time can reduce the water saturation and the water blocking damage of the reservoir. Besides, OSSF is also beneficial to the flow back of invasive external fluid in a reservoir.

3.4 Mechanism analysis

3.4.1 Physical blocking

Figure 12 shows that aggregates can be formed when the concentration exceeds its critical micelle concentration (CMC). Adjusting the OSSF concentrations to match reservoir needs with varied pore and throat sizes is necessary when the aggregates invade reservoir with external fluids. This causes friction to form on the surface in which pores or throats and fluid come in contact with each other.

When the aggregates move into the pores or throats of reservoirs, as shown in **Figure 13(b)**, the interfacial tensions on the two contact surfaces are even. When the aggregates flow from the pores to the reservoir throats (**Figure 13(c)**), friction can decrease the flow rate. When aggregates move from the throats to the pores (**Figure 13(d)**), the interfacial tension between aggregates and external fluid becomes smaller. In the process of production, the fluid begins to flow back, the aggregates move back from the throats to the pores, and then, the differences in the interfacial tensions between two contact surfaces could become the driving force for flowing, which could accelerate these fluids to flow back.

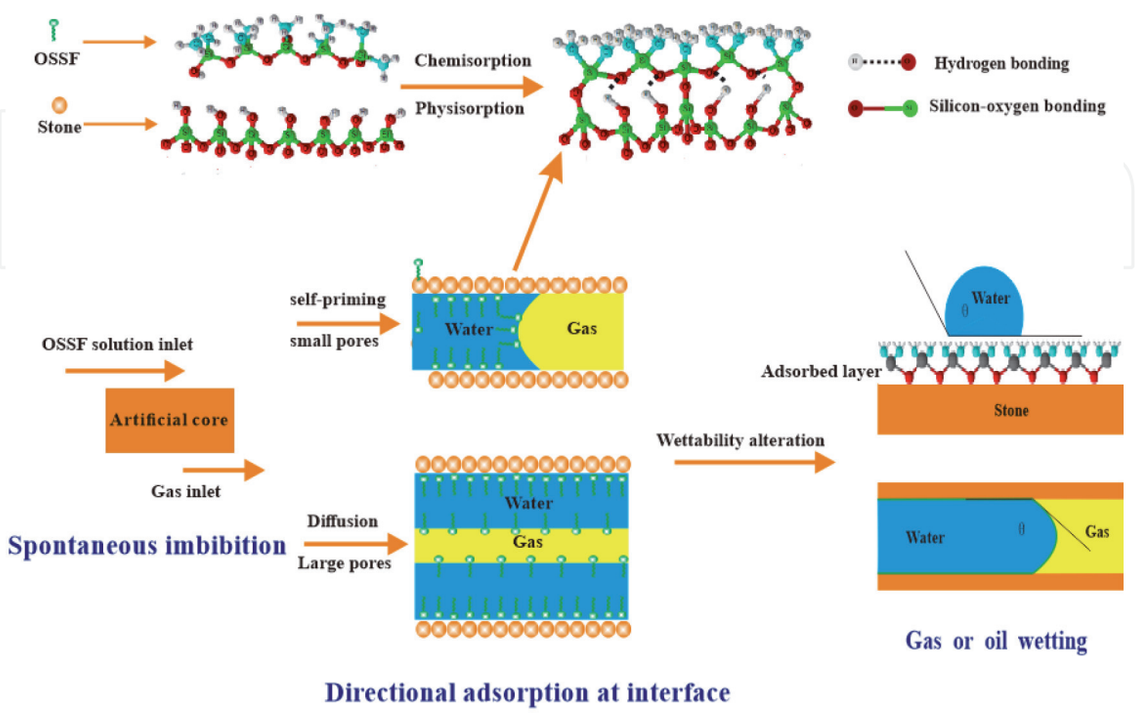

Figure 14.
Principle diagram of OSSF adsorption on water-pore interface.

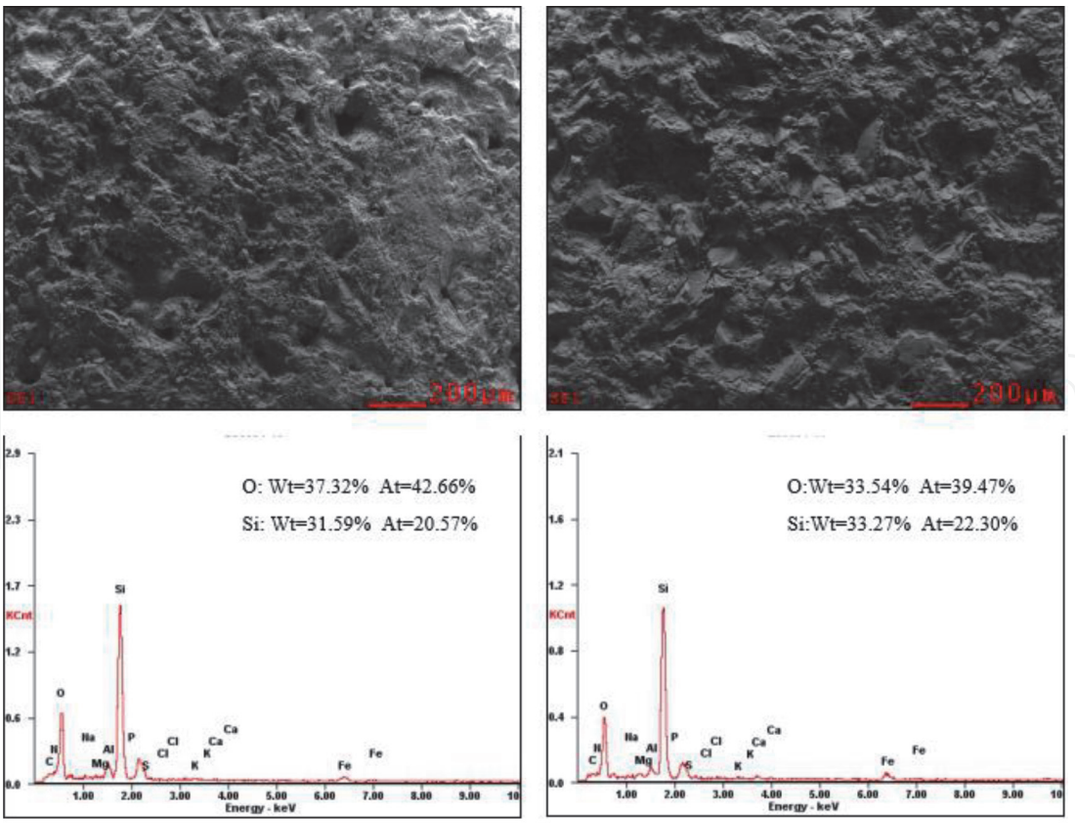

Figure 15.
SEM image and X-ray spectrum of artificial cores. (a) Untreated and (b) treated by 0.20 wtT OSSF.

3.4.2 Wettability alteration

When the alkaline solution invades into the reservoir, the structural groups of the silicon-oxygen bond (Si-O-Si) on the surface of the silicate minerals can produce silanol groups (Si-OH) by hydrolysis. The density can reach up to 6–7 nm per square. These silanol groups can adsorb the water molecules owing to the hydrogen bonding and the Van Der Waals force upon the water-pore interface. Within both forces, hydrogen bonding plays an important role. It is needed to overcome the adhesion force between rock and water, thereby decreasing the remaining water in the formation [25]. The basic structural unit of the OSSF is polydimethylsiloxane. The silicon-oxygen chain is the polar part of the OSSF composition, and the methyl group represents the nonpolar part.

Under high temperature and catalyst conditions, polarization occurs in the silicon oxygen main chain. This leads to multipoint adsorption of silanol groups (Si-OH) and silicon-oxygen bond (Si-O-Si) through chemical bonding and hydrogen bonding. Meanwhile, the methyl groups directionally rotate and sequentially arrange on the rock surface. This process is shown in **Figure 14** [26]. These directionally adsorbed methyl groups reduce the surface energy of the rock and lead to the hydrophobization on the rock surface, changing the composition of the rock surface. Meanwhile, the capillary force direction of fluids and the physical properties of the gas reservoir change [17].

As shown in **Figure 15**, the cores treated by OSSF have a higher weight and atom Si number as well as a lower weight and atom O number. This is because the cores are composed of silicon and oxygen, with a chemical structural much like that of OSSF. **Figure 16** shows how the OSSF adsorption on the reservoir core surface can

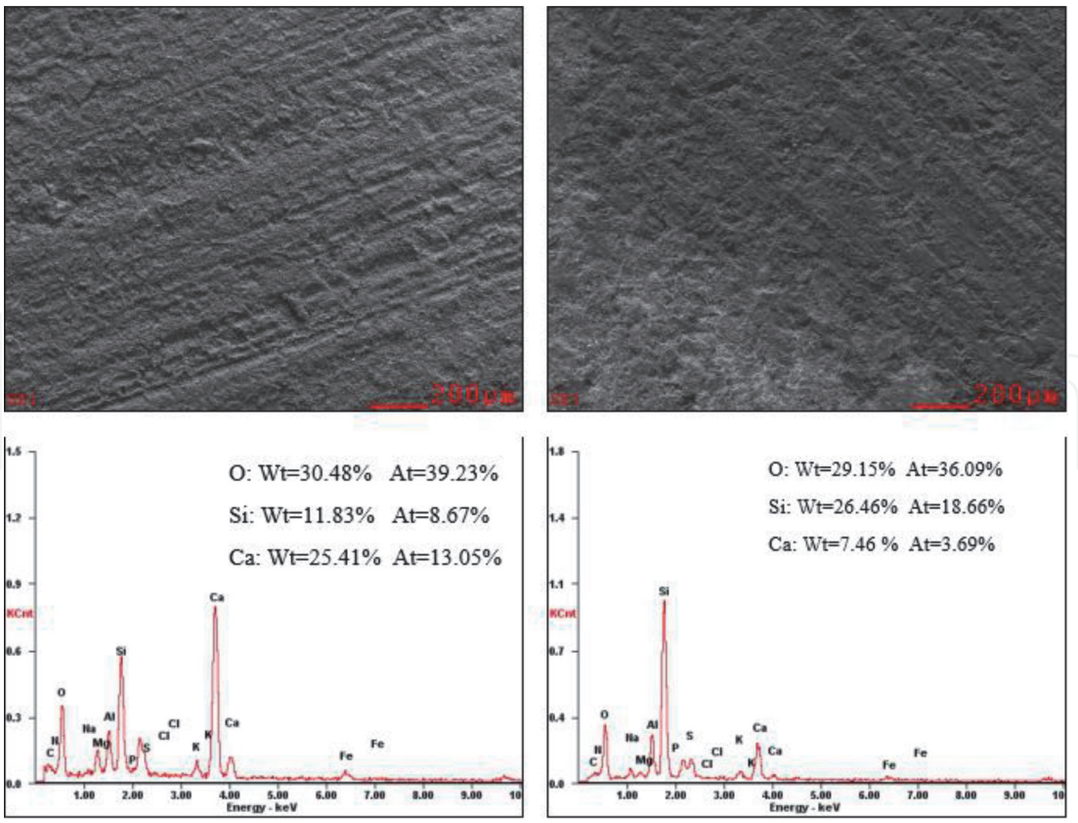

Figure 16.
SEM image and X-ray spectrum of reservoir cores. (a) Untreated and (b) treated by 0.20 wt% OSSF.

significantly increase the weight and number of atom Si and Ca but slightly decrease that of atom O. Since we use carbonate cores, their surface components change greatly as a result of OSSF adsorption. Both artificial and reservoir core surfaces show more Si atoms. The outermost areas of the core are composed of Si-CH_3, and the cores have become hydrophobic.

3.4.3 Adsorption energy

The weak interaction among the molecules can be calculated accurately by the computational technique based on quantum chemistry. In this paper, (a) silicon-oxygen tetrahedron and (b) dimethyl siloxane were applied to simulate the surface of the untreated cores and OSSF treated cores, respectively. The oxygen atoms at the edge were saturated with hydrogen atoms.

Gaussian 09 W software (Gaussian Inc., Wallingford, CT, USA) is used as the simulation tool, and 6-31G is selected as the basic set. Correction is performed using a basis set superposition error (BSSE). In the adsorption system, the distance between the C atoms of methane and the O atoms of water is the equilibrium distance r_e. The following Eqs. (3) and (4) were used to calculate the adsorption energies (E_e) of water and methane on the core surface [27, 28]:

$$E_e = E_{CH_3-Si//CH_4/Si-O//CH_4} - E_{Si-O/CH_3-Si} - E_{CH_4} \quad (3)$$

$$E_e = E_{CH_3-Si//H_2O/Si-O//H_2O} - E_{Si-O/CH_3-Si} - E_{H_2O} \quad (4)$$

Here, $E_{CH_3-Si//CH_4/Si-O//CH_4}$ represents the system energy in kJ/mol when silicon-oxygen tetrahedron and dimethyl siloxane adsorb methane. $E_{CH_3-Si//H_2O/Si-O//H_2O}$ represents the system energy when silicon-oxygen tetrahedron and dimethyl siloxane adsorb water in kJ/mol. E_{Si-O/CH_3-Si} is the energy of silicon-oxygen tetrahedron or dimethyl siloxane in kJ/mol. E_{H_2O/CH_4} represents the energy of water or methane in kJ/mol.

As shown in **Figure 17** and **Table 4**, the distances of the dimethyl siloxane models between CH_4 and H_2O are larger or similar than that of silicon-oxygen tetrahedron. The adsorption energy of silicon-oxygen tetrahedron and the dimethyl siloxane models to CH_4 is 11.21 and 0.46 kJ/mol, respectively, which indicates that the adsorption of methane on the core surfaces is nonhydrogen-bonding physical adsorption. The adsorption energy of silicon-oxygen tetrahedron and the dimethyl siloxane models to H_2O is 81.78 and 52.18 kJ/mol, respectively, suggesting the adsorption of water is hydrogen-bonding adsorption. Since the adsorption binding energy of CH_4 and H_2O on the silicon-oxygen tetrahedron model is higher than that on the dimethyl siloxane model, the stability of CH_4 and H_2O adsorbed on the pore surface of cores treated by OSSF is lower than that on the untreated cores. At the same flow-back pressure, CH_4 and H_2O adsorbed on the surface of treated cores are often more easily desorbed. Under the same temperature and pressure conditions, after the adsorption of OSSF, the affinity and adhesion of the rock surface to CH_4 and H_2O are reduced, leading to the reduction of the shear stress of CH_4 and H_2O on the pore surfaces of the reservoir, when gas or external fluids flow in the reservoir [29]. This can increase the fluidity of CH_4 and H_2O and finally improve the permeability of CH_4 and H_2O, thereby decreasing water saturation of the reservoir.

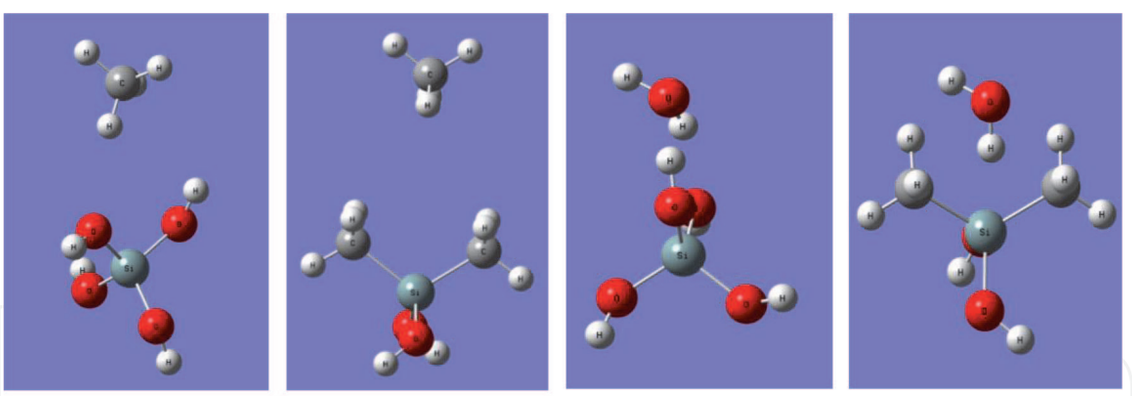

(a) (b) (c) (d)

Figure 17.
Optimized structure of the models absorbed the CH_4 as shown in (a) and (b) and H_2O as shown in (c) and (d) (T = 273.15 K, P = 1 atm).

Adsorption model	Adsorbate	r_e/ (nm)	E_e/ (kJ·mol^{-1})
Silicon-oxygen tetrahedron (a)	CH_4	4.33	−11.21
	H_2O	3.32	−81.77
Dimethylsiloxane (b)	CH_4	5.17	−0.46
	H_2O	3.17	−52.18

Table 4.
Adsorption equilibrium distance (r_e) and adsorption energy (E_e) of the absorbed the CH_4 and H_2O (T = 273.15 K, p = 1 atm).

4. Conclusions

1. An ultralow surface tension could be obtained using OSSF. A 0.20 wt% OSSF solution can alter cores from water wetting to preferential gas wetting.

2. OSSF can remarkably decrease the water saturation and spontaneous imbibition rate of cores, resulting in a reduction in the cores' water blocking damage rate. In this case, the effect of cores' wettability alteration to water saturation and the spontaneous imbibition rate is higher.

3. In the gas driven flow-back experiment, OSSF improved core permeability recovery. The remaining water saturation was also found to be low.

4. The main mechanism for improving core permeability includes the physical obstruction effect, surface tension reduction, and adsorption energy reduction, as well as the capillary force, adhesion, and shear stress of methane and liquid on rock surfaces.

Acknowledgements

This work was supported by the National Major Science and Technology Project of China (Nos. 2016ZX05051, 2016ZX05052, and 2016ZX05030) and Research on Qaidam's Excellent Drilling and Completion Technology (2016E-0109).

Conflicts of interest

The authors declare that there is no conflict of interest regarding the publication of this paper.

Author contributions

The supervisor, Jie Zhang, conducted the experimental work and analyzed the results of the research. All authors contributed to the analysis of results. Jie Zhang wrote the manuscript. Xu-Yang Yao contributed to experiment's design and analysis of the results. Bao-Jun Bai contributed to analysis and discussion of the results, reviewing, and editing of the manuscript.

DOI: http://dx.doi.org/10.5772/intechopen.90811

Author details

Jie Zhang[1,3*], Xu-Yang Yao[2], Bao-Jun Bai[3] and Wang Ren[1]

1 Drilling Fluids Research Department, CNPC Engineering Technology R&D Company Limited, Beijing, P.R. China

2 Petrochina Xin Jiang Oil Field Company, Karamay, P.R. China

3 Department of Petroleum Engineering, Missouri University of Science and Technology, Rolla, MO, USA

*Address all correspondence to: zhangjiedri@cnpc.com.cn

References

[1] Zhong XY, Huang L, Wang LH. Research progress on water blockage effect in low permeability gas reservoirs. Special Oil & Gas Reserves. 2008;**15**: 12-23

[2] He CZ, Hua MQ. Quantitative study of water blocking mechanism. Drilling Fluid & Completion Fluid. 2000;**3**:4-7

[3] Pham VP, Jo YW, Oh JS, Kim SM, Park JW, Kim SH, et al. Effect of plasma-nitric acid treatment on the electrical conductivity of flexible transparent conductive films. Japanese Journal of Applied Physics. 2013;**52**: 075102

[4] Liu M, Wu Q. Research progress and prospect of water blocking agent. Guangzhou. Chemistry & Industry. 2013;**41**:32-42

[5] Nasr-EI-Din HA, Lynn JD, AI-Dossary KA. Formation damage caused by a water blockage chemical: Prevention through operator supported test programs. SPE. 2002;**33**:297-325

[6] Zhang WB, Li CF, Shi XW. Application of alcoholic acid acidification in Qinghai oil field. Oilfield Chem. 2009;**26**:24-28

[7] Bai FL. Water phase trapping damage and the study of relieving measures in gas reservoir. Petrochemical Industry Application. 2010;**29**:14-17

[8] Bang V, Pope G, Sharma M, Baran JR Jr. Development of a successful chemical treatment for gas wells with water and condensate blocking damage. In: SPE Annual Technical Conference and Exhibition, New Orleans, Louisiana, 4–7 October 2009. Paper SPE 124977. 2009

[9] Bang VSS, Yuan CW, Pope GA, Baran JR Jr, Skildum J. Improving productivity of hydraulically fractured gas condensate wells by chemical treatment. In: OSSFhore Technology Conference, Houston, Texas, 5–8 May 2008. Paper OTC 19599. 2008

[10] Bang V, Pope G, Mukul M, Baran JR Jr, Ahmadi M. A new solution to restore productivity of gas Wells with condensate and water blocks. In: SPE Annual Technical Conference and Exhibition, Denver, Colorado, 21–24 September 2008. SPE 116711. 2008

[11] Li YY, Jiang GC, Xuan Y. Synthesis and performance evaluation of drilling fluid anti-blockage agent of low porosity and low permeability reservoir. Drilling Fluid and Completion Fluid. 2014;**31**: 9-12

[12] Li XQ, Wang YC, Wang YQ. Experimental study on the effect of mixed surfactants on water blockage. Chemistry & Bioengineering. 2013: 85-89

[13] Liu Y, Guo L, Bi K, Ren W, Liu L, Li YG, et al. Synthesis of cationic gemini surfactant and its application in water blocking. Fine and Specialty Chemicals. 2011;**19**:8-10

[14] Liu XF, Kang YL, Luo PY, You LJ, Tang Y, Kong L. Wettability modification by fluoride and its application in aqueous phase trapping damage removal in tight sands to ne reservoirs. Journal of Petroleum Science and Engineering. 2015;**133**:201-207

[15] Zhang XQ. Researching on the use of new type surfactant to weaken water blocking and jamin effect. Master thesis. Qingdao, China: Ocean Univ. China; 2013

[16] Yin D, Luo P, Zhang J. Synthesis of Oligomeric silicone surfactant and its interfacial properties. Applied Sciences. 2019;**9**(3):497

[17] Jiang GC, Wei YJ, Zhang M, Luo SJ, Yang Z, Pang JT. Review of evaluation methods to gas wettability. Science Technology & Engineering. 2012;**13**: 5562-5565

[18] Owens DK, Wendt RC. Estimation of the surface free energy of polymers. Journal of Applied Polymer Science. 1969;**13**:1741-1747

[19] Dong B, Lan L, Cheng ZH, Xia HY, Niu J. Study on capillary self-absorption characteristics of dense gas reservoir rocks. Drilling and Production Technology. 2012;**35**:34-37

[20] Lai NJ, Ye ZB, Liu XJ, Yang JJ, Zhang JF. Study on water blocking damage in low permeability tight sandstone gas reservoir. Natural Gas Industry. 2005;**25**:125-127

[21] Stand. Adm. China. Determination Method of Relative Permeability of Two-Phase Fluids in Rocks (GB/T 28912–2012). Beijing, China: China Stand. Press; 2012

[22] Guo TS, Li TW, Li HB. Laboratory study of water locking damage under imbibition in volcanic gas reservoirs. Science Technology & Review. 2011;**29**: 62-66

[23] Bennion DB, Thomas FB, Ma T. Formation damage processes reducing productivity of low permeability gas reservoirs. In: SPE Rocky Mountain Regional/Low Permeability Reservoirs Symposium and Exhibition, Denver, Colorado, 12–15 March 2000. Paper SPE 60325. 2000

[24] Bennion DB, Bietz RF, Thomas FB. Reductions in the productivity of oil and gas reservoirs due to aqueous phase trapping. Petroleum Society of Canada. 1994;**33**:45-54

[25] Wu JF, Wu DQ. Surface ionization and complexation of mineral-water interface. Advances in Earth Science. 2000;**1**:90-96

[26] Cao Y, Li HL. Adsorption behavior of polymeric surfactants at solid-liquid interface. Acta Physico-Chimica Sinica. 1999;**10**:895-899

[27] Koretsky CM, Sverjensky DA, Sahai N. A model of surface site types on oxide and silicate minerals based on crystal chemistry. Implications for site types and densities, multi-site adsorption, surface infrared spectroscopy, and dissolution kinetics. American Journal of Science. 1998;**298**: 349-438

[28] Castro EAS, Gargano R, Martins JBL. Theoretical study of benzene interaction on kaolinite. Computer-Aided Materials Design. 2012;**112**:2828-2831

[29] Taghvaei E, Moosavi A, Nouri-Borujerdi A. Superhydrophobic surfaces with a dual-layer micro-and nanoparticle coating for drag reduction. Energy. 2017;**12**:1-10